Erzincan Üniversitesi
Fen Bilimleri Enstitüsü Dergisi
2021, 14(2),857-863
ISSN: 1307-9085, e-ISSN: 2149-4584
Araştırma Makalesi

Erzincan University
Journal of Science and Technology
2021, 14(2),857-863
DOI: 10.18185/erzifbed.949658
Research Article

The S^{4}G Sample: Absorption Properties of AGNs with *WISE*, 3XMM, and FIRST/NVSS

Tuba İkiz[1]

[1]Atatürk University Astrophysics Research and Application Center (ATASAM), Erzurum, Turkey

Geliş / Received: 08/06/2021, Kabul / Accepted: 31/08/2021

Abstract

In this study, mid-infrared colours were calculated by İkiz et al. (2020) at IRAC 3.6 and 4.5 and *WISE* 3.4 and 4.6 μm from the *Spitzer* Stellar Structure Survey in Galaxies – S^{4}G sample consisting of more than 2500 galaxies, in addition to its extension, from a sample of 400 galaxies were examined in X-ray 3XMM-DR5 and in radio VLA NVSS and FIRST archives to find their counterparts and classified as radio-loud and radio-quiet active galactic nuclei based on their activity. The absorption properties of galaxies were determined according to the hardness ratios.

Key words: galaxies: active – infrared: galaxies – radio continuum: galaxies – X-rays: galaxies

S^{4}G Örneklemesi: *WISE*, 3XMM ve FIRST/NVSS ile AGN'lerin Soğurma Özellikleri

Öz

Bu çalışmada, 2500'den fazla galaksiden oluşan Galaksilerdeki Yıldız Yapılarının *Spitzer* Araştırması (S^{4}G) örneklemesine ek olarak onun uzantısı 400 galaksiden oluşan örneklemeden IRAC 3.6 ve 4.5 ve *WISE* 3.4 ve 4.6 μm de orta-kırmızı öte renkleri İkiz vd. (2020) tarafından hesaplanmış galaksiler hem XMM-Newton hem de radyo arşivlerde taranarak eşlenikleri bulunmuş ve aktivitelerine dayanarak, radyo-gürültülü ve radyo-sessiz aktif galaktik çekirdekler olarak sınıflandırılmıştır. Galaksilerin soğurma özellikleri sertlik oranlarına göre belirlenmiştir.

Anahtar Kelimeler: galaksiler: aktif – kırmızı öte: galaksiler - radyo süreklilik: galaksiler – X-ışınları: galaksiler

1. Introduction

Active galactic nuclei (AGN) are amongst the most powerful sources in the universe. Luminosity ranging from AGN in nearby galaxies emitting at luminosities of about 1040 erg s^{-1} , to distant quasars emitting >1047 erg s^{-1}. Active galactic nuclei play a crucial role for understanding the accretion history of the universe as well as galaxy evolution (e.g. Caputi, 2014), and in the growth of supermassive black holes (Fabian and Iwasawa, 1999). There is a connection between black hole growth and galaxy growth. This is shown both by the tight correlation between blackhole mass and galaxy bulge mass (e.g. Magorrian et al., 1998; Ferrarese and Merritt, 2000; Gebhardt et al., 2000).

X-ray and mid-IR emission are very good tools of accretion in AGN. AGN central region is considered to be surrounded by an optically thick molecular torus and large masses of dust

*Corresponding Author: tubaaaikiz@gmail.com

associated with this torus reprocess the X-ray and UV emission from the accretion disk and reradiate it in the mid infrared (MIR) wavelengths (Pier and Krolik, 1993).

Luminous AGNs show a red MIR power-law spectral energy distribution (SED), which is dominated by thermal emission from hot dust (Neugebauer et al., 1979; Elvis et al., 1994; Rieke and Lebofsky, 1981). Using mid-infrared colours and X-ray HR cuts are extremely successful in defining the properties of QSO-like and bright Seyfert-type sources. These sources can not include fainter galaxies that AGN emission can not be seperate strictly and besides that radiatively inefficient (LINER or LERG) sources where most of the energy is released through a jet, rather than as radiative output (see e.g. Hardcastle et al., 2009; Best and Heckman, 2012; Mingo et al., 2014; Mingo et al., 2016). It is also significant to keep in sight that a strict HR cut can eliminate sources with a soft excess, most serendipitously radio-loud AGN, where jet-related emission produces soft X-rays (Mingo et al., 2016).

The AGN are grouped into two classes, unabsorbed (type-1) and absorbed (type-2), depending on their optical spectroscopic classification and X-ray absorption properties, using hardness ratios. Sources for which optical spectroscopy does not allow a clear distinction between type-1 and type-2 are classified using their hardness ratios. An AGN with a hardness ratio HR < -0.2 is called type-1, and with HR > -0.2 type-2 (Hasinger, 2018).

2. Material and Method

In this study, sources from the *Spitzer* Stellar Structure Survey in Galaxies – S^{4}G (see Sheth, et al., 2010 for the full survey description) were used, confirmed by mid-infrared color measurement and the Wide-field Infrared Survey Explorer (*WISE*) all-sky survey by İkiz, et al., (2020), and these sources were also studied in X-rays (3XMM DR5) and radio (Faint Images of the Radio Sky at Twenty centimetres – FIRST/NRAO VLA Sky Survey – NVSS). The *WISE* instrument has mapped the whole sky in four infrared bands W1 and W2 centered at 3.4 and 4.6 μm. S^{4}G galaxies that are *WISE* [W1–W2] and the *Spitzer* Infrared Array Camera (IRAC) [3.6]-[4.5] central colours detected by İkiz et al., (2020) have been used to find their counterparts in both X-ray and radio.

X-ray data from the archive of *XMM-Newton* survey which has a large field of view of 30′ thus providing a major resource, a deep, large-area sky survey is used. In this study, AGN candidate counterparts are identified in 3XMM-DR5 (Rosen, et al., 2016) catalogue within 30′. All compact X-ray sources with a luminosity above $\approx 10^{42}$ erg s^{-1}(2-10 keV) are considered to be AGN. X-ray survey with *XMM-Newton* at energies < 10 keV are sensitive to all but the most heavily obscured AGN.

Radio data from the low-resolution (45′) VLA NVSS, and the high-resolution (5′) VLA FIRST survey are used. Astronomical Resource Cross-matching for High Energy Studies (ARCHES) catalogue thanks to Mingo, et al., (2016) which has FIRST+NVSS combined radio fluxes is used to investigate the radio continuum counterparts within 30′ radius search. The existence of a compact radio core especially is a good indicator of the presence of an AGN, since its radio emission is mostly from nonthermal origin, that is, not related to star formation (Ho, 1999). Radio surveys are sensitive and generally have very accurate positional information.

3. Results and Discussion

In this study, the S^{4}G sample 170 galaxies; both X-ray and radio counterparts in related archives are detected and classified using activity Table 1, and also combined 1.4 GHz radio flux (in mJy) to the X-ray flux and HR ratios are obtained. These galaxies *Spitzer* and *WISE* colors have been measured by İkiz et al., (2020) study and now their absorption properties are examined.

Table 1. Activity table based on Mingo et al., (2016).

Label	***WISE* colour selection**	**Mid-IR/Optical**	**X-rays**	**Radio**
Elliptical	W1-W2 < 0.5; 0 < W2-W3 < 1.6	Elliptical galaxy (isolated) Elliptical galaxy (cluster) LINER	Rad. inefficient AGN Hot ICM gas	LERG
Spiral	W1-W2 < 0.5; 1.6 ≤ W2-W3 < 3.4	Star-forming galaxy Star-forming galaxy + AGN	Star formation Seyfert galaxy	Star formation Low-L NLRG LERG
Starburst	W1-W2 < 0.5; W2-W3 ≥ 3.4	Starburst galaxy ULIRG	Star formation Seyfert galaxy	Star formation Low-L NLRG
AGN/QSO	W1-W2 ≥ 0.5; W2-W3 < 4.4	AGN	Luminous Seyfert galaxy BL-Lac QSO	NLRG BLRG QSO

Notes. For each of our source types, selected on the *WISE* color/color plot, this table shows the types of activity most likely to be found at each wavelength. For each color category, several combinations of the elements in columns 2-4 may be possible; for example, in the first group, an elliptical galaxy in a cluster, with a radiatively inefficient AGN in X-rays, and an LERG in radio. LINER stands for low-ionization nuclear emission-line region. ULIRG stands for ultraluminous infrared galaxy. QSO stands for quasars. LERG stands for low-excitation radio galaxy; high-excitation sources (HERG) include NLRG (narrow-line radio galaxies), and BLRG (broad-line radio galaxies).

Normally, it is preferable to use net (background) counts rather than fluxes to calculate HR. However, due to the nature of the X-ray catalogue, multiple observations can be made with multiple instruments for a given source, so it was decided to use average (all observations for all sources) net fluxes, as was done in the Mingo et al., (2016) study.

The hardness ratio (HR) use is defined as:

$$HR = (H - S) / (H + S)$$

where S and H are the count ratios of soft (S) and hard (H) bands, respectively.

$$HR = (F_{2\text{-}12keV} - F_{0.2\text{-}2keV})/(F_{2\text{-}12keV} + F_{0.2\text{-}2keV})$$

Figure 1 and 2 show the distribution of hardness ratios for all the sources on the Y axis, and the ratio of the radio to the relative X Ray (soft and hard, respectively) flux on the X axis. In this way, the 'radio loudness' and 'X-ray loudness' of the sources are defined easily. The general trend changes according to the ratio of hard or soft X-ray fluxes used in the x-axis. For soft X-rays (Fig. 1) the ratio seems quite constant as evidenced by the picking of sources around a vertical line at $F_{(1,4\ GHz)} / F_{(0,2\text{-}2)\ keV} \sim 10^{14}\text{-}10^{15}$, especially with some outliers situated on the left side of the graph (larger relative X-ray fluxes). For hard X-rays (Fig. 2) the

situation is somewhat different and there seems to be a slight negative trend between the radio/hard X-ray flux and the hardness ratio, i.e. more 'hard X-ray loud' (less 'radio-loud') sources have harder spectra.

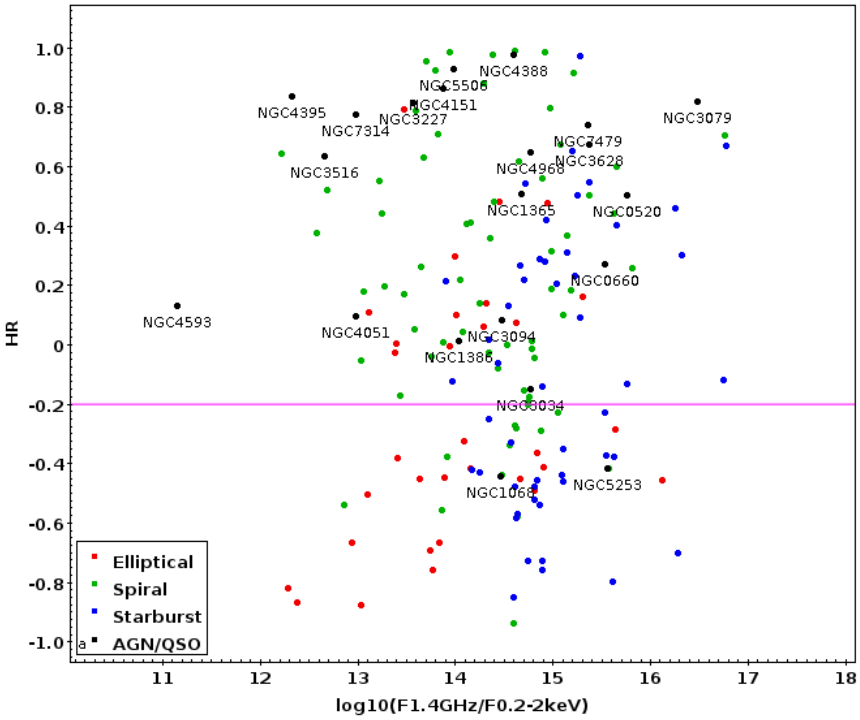

Figure 1. X-ray hardness ratio versus ratio of the 1.4 GHz radio flux (mJy) to X-ray flux (soft, 0.2-2 keV, erg $cm^{-1}s^{-1}$). The pink solid line indicates the HR (= -0.2) limit.

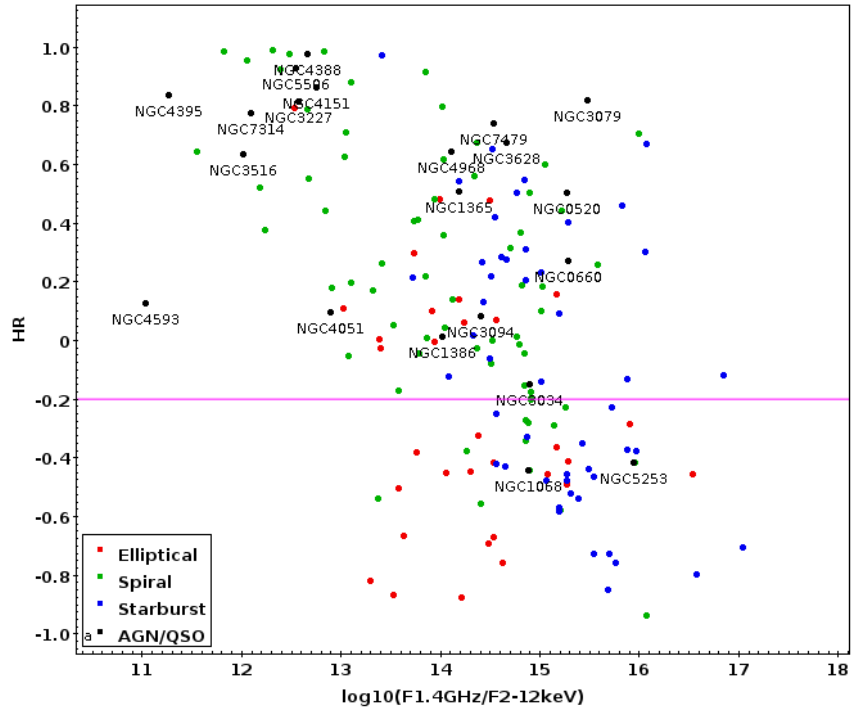

Figure 2. X-ray hardness ratio versus ratio of the 1.4 GHz radio flux (mJy) to X-ray flux (hard, 2-12 keV, erg $cm^{-1}s^{-1}$). The pink solid line indicates the HR (= -0.2) limit.

HR values are higher than -0.2 so it can be used as a threshold to distinguish between X-ray absorbing and non-X-ray absorbing sources. AGNs show the widest distribution of all populations and also have the largest HR ratios and are located on the 'X-ray louder' side of both the soft and hard X-ray HR plots.

The AGN are grouped into two classes, unabsorbed (type-1) and absorbed (type-2). An AGN with a hardness ratio HR < -0.2 is called type-1, and with HR > -0.2 type-2. The classical distinction between optically unobscured (type-1) and obscured (type-2) AGN is done using a discrimination through optical spectroscopy. Optical type-1 AGN have broad permitted emission lines (>2000 km/s), while optical type-2 AGN do not show broad permitted lines, but still have high excitation narrow emission lines (Hasinger, 2018).

Therefore, many studies essentially use the existence of broad lines as discriminatory and categorize objects as type-1 AGN only if they have broad lines (BLAGN, see e.g. Barger et al., 2005; Treister and Urry, 2006). This classification also has the advantage that it can be applied to sources without spectroscopic information but with reliable photometric redshifts (Hasinger, 2018). With 21 red nuclei detected by *Spitzer* and *WISE*, the AGN has both X-ray and radio fluxes. As shown in Table 1, 2 galaxies have HR values smaller than -0.2, associated with unabsorbed spectra (BLAGN), and the rest 19 have larger hardness ratios. In addition, the [3.6]-[4.5] and [W1]-[W2] colors of these AGNs, together with their morphological types, are given in Table 2, and it is seen that all of them are red coloured AGNs. Note that many (but not all) of the brightest hard X-ray sources are identified as AGN candidates by the *WISE* criterion and also by their IRAC colors. One note that a less stringent red color cut, for instance 0.3 instead of 0.5, undoubtedly yields more AGN candidates (İkiz et al., 2020).

Table 2. Detected 21 AGNs in both 3XMM-DR5 and ARCHES catalogues given with *Spitzer* and *WISE* colours measured by İkiz et al., (2020) and HR values estimated in this study.

Galaxy **(1)**	**RA** (deg) **(2)**	**DEC** (deg) **(3)**	**TT** **(4)**	**[3.6]-[4.5]** (mag) **(5)**	**Error** (mag) **(6)**	**[W1]-[W2]** (mag) **(7)**	**Error** (mag) **(8)**	**[W2]-[W3]** (mag) **(9)**	**Error** (mag) **(10)**	**HR** **(11)**
NGC 0520	21.14538	3.79159	1.3	0.522	0.043	0.752	0.016	4.207	0.013	0.5
NGC 0660	25.75969	13.64581	1.3	0.568	0.026	1.189	0.007	3.220	0.006	0.3
NGC 1068	**40.66962**	**-0.01331**	**3.0**	**0.797**	**0.017**	**1.116**	**0.006**	**2.744**	**0.005**	**-0.4**
NGC 1365	53.40155	-36.14039	3.2	0.679	0.020	0.800	0.006	3.587	0.005	0.5
NGC 1386	54.19239	-35.99920	-0.7	0.783	0.033	0.965	0.011	3.289	0.009	0.0
NGC 3034	148.96800	69.67975	7.5	0.690	0.013	1.453	0.004	2.351	0.004	-0.1
NGC 3079	150.49090	55.67988	6.6	0 .317	0.031	0.510	0.010	3.676	0.009	0.8

NGC 3094	150.35812	15.77011	1.1	0.950	0.028	1.549	0.008	2.513	0.006	0.1
NGC 3227	155.87740	19.86513	1.5	0.590	0.026	0.775	0.011	3.287	0.009	0.8
NGC 3516	166.69780	72.56850	-2.0	0.519	0.035	0.825	0.009	2.593	0.009	0.6
NGC 3628	170.07064	13.58899	3.1	0.484	0.040	0.641	0.011	3.825	0.010	0.7
NGC 4051	180.79007	44.53131	4.0	0.748	0.030	0.931	0.018	3.126	0.015	0.1
NGC 4151	182.63561	39.40578	2.0	0.988	0.029	1.233	0.010	2.699	0.009	0.9
NGC 4388	186.44490	12.66209	2.8	0.855	0.033	1.114	0.020	3.108	0.016	1.0
NGC 4395	186.45360	33.54686	8.9	0.462	0.114	0.766	0.100	2.987	0.091	0.8
NGC 4593	189.91437	-5.34414	3.0	0.667	0.035	0.816	0.020	2.800	0.018	0.1
NGC 4968	196.77420	-23.67690	-2.0	0.744	0.045	0.995	0.018	3.844	0.014	0.6
NGC 5253	**204.98315**	**-31.64006**	**8.9**	**1.298**	**0.027**	**1.852**	**0.011**	**3.991**	**0.007**	**-0.4**
NGC 5506	213.31209	-3.20757	1.2	1.059	0.029	1.292	0.011	2.591	0.009	0.9
NGC 7314	338.94252	-26.05043	4.0	0.712	0.047	0.804	0.018	2.912	0.017	0.8
NGC 7479	346.23590	12.32293	4.3	1.150	0.041	1.449	0.015	3.735	0.011	0.7

Notes. Columns are: (1) Galaxy name; (2) Right ascension (J2000); (3) Declination (J2000); (4) Numerical morphological type; (5) [3.6]-[4.5] color (İkiz et al., 2020); (6) [3.6]-[4.5] color error (İkiz et al., 2020); (7) [W1]-[W2] color (İkiz et al., 2020); (8) [W1]-[W2] color error (İkiz et al., 2020); (9) [W2]-[W3] color (İkiz et al., 2020); (10) [W2]-[W3] color error (İkiz et al., 2020); (11) Hardness ratio

References

Best, P. N., Heckman T. M., 2012. On the fundamental dichotomy in the local radio-AGN population: accretion, evolution and host galaxy properties, Monthly Notices of the Royal Astronomical Society, 421, 1569.

Caputi, K. I., 2014. Active galactic nuclei and their role in galaxy evolution: The infrared perspective, International Journal of Modern Physics D, 23, 1430015.

Elvis M. et al., 1994. Atlas Of Quasar Energy Distributions, The Astrophysical Journal Supplement Series, 95:1-68.

Fabian, A. C., Iwasawa K., 1999,. The mass density in black holes inferred from the X-ray background, Monthly Notices of the Royal Astronomical Society, 303, L34.

Ferrarese, L. & Merritt, D. 2000. A Fundamental Relation Between Supermassive Black Holes And Their Host Galaxies, The Astrophysical Journal, 539:L9–L12.

Gebhardt K., et al., 2000. A Relationship between Nuclear Black Hole Mass and Galaxy Velocity Dispersion, The Astrophysical Journal, 539, L13.

Hardcastle, M. J., Evans D. A., Croston J. H., 2009. The active nuclei of z < 1.0 3CRR radio sources, Monthly Notices of the Royal Astronomical Society, 396, 1929.

Hasinger, G., 2018. Absorption properties and evolution of active galactic nuclei, Astronomy and Astrophysics, 490, 905-922.

Ho, L. C., 1999. The Spectral Energy Distributions of Low-Luminosity Active Galactic Nuclei, The Astrophysical Journal, 516, 672.

İkiz, T., Peletier, R.F., Barthel, P., et al. 2020. Infrared-detected AGNs In The Local Universe, Astronomy and Astrophysics, 640, A68.

Magorrian, J., Tremaine, S., Richstone, D., et al. 1998. The Demography Of Massive Dark Objects In Galaxy Centers, The Astronomical Journal, 115:2285-2305.

Mingo, B., et al., 2014. An X-ray survey of the 2 Jy sample – I. Is there an accretion mode dichotomy in radio-loud AGN?, Monthly Notices of the Royal Astronomical Society, 440, 269.

Mingo, B., et al., 2016. The MIXR sample: AGN activity versus star formation across the cross-correlation of WISE, 3XMM, and FIRST/NVSS, Monthly Notices of the Royal Astronomical Society, 462, 2631–2667.

Neugebauer G., Oke J. B., Becklin E. E., Mathews K., 1979. Absolute Spectral Energy Distribution Of Quasi-stellar Objects From 0.3 To 10 Microns, The Astrophysical Journal, 230: 79-94.

Pier, E. A., Antonucci, R., Hurt, T., Kriss, G., & Krolik, J., 1994. The intrinsic nuclear spectrum of NGC 1068, The Astrophysical Journal, 428, 124-129.

Rieke, G. H., & Lebofsky, M. J. 1981. Spectral Components Of NGC 4151, The Astrophysical Journal, 250:87-97.

ARCHES Catalogue.

http://www.arches-fp7.eu/arches/index.php?option=com_content&view=article&id=1&Itemid=101

3XMM-DR5 Catalogue.

http://xmmssc.irap.omp.eu/Catalogue/3XMM-DR5/3XMM_DR5.html